CHALMERS
UNIVERSITY OF TECHNOLOGY

Predicting Electric Vehicle Energy Consumption from Field Data Using Machine Learning

Predicting Electric Vehicle Energy Consumption from Field Data Using Machine Learning

Qingbo Zhu, Yicun Huang, Chih Feng Lee, *IEEE Senior Member*, Peng Liu, *IEEE Member*, Jin Zhang, Torsten Wik, *IEEE Member*

***Abstract*—This study addresses the challenge of accurately forecasting the energy consumption of electric vehicles (EVs), which is crucial for reducing range anxiety and advancing strategies for charging and energy optimization. Despite the limitations of current forecasting methods, including empirical, physics-based, and data-driven models, this paper presents a novel machine learning-based prediction framework. It integrates physics-informed features and combines offline global models with vehicle-specific online adaptation to enhance prediction accuracy and assess uncertainties. Our framework is tested extensively on data from a real-world fleet of EVs. While the leading global model, quantile regression neural network (QRNN), demonstrates an average error of 6.30%, the online adaptation further achieves a notable reduction to 5.04%, with both surpassing the performance of existing models significantly. Moreover, for a 95% prediction interval, the online adapted QRNN improves coverage probability to 91.27% and reduces the average width of prediction intervals to 0.51. These results demonstrate the effectiveness and efficiency of utilizing physics-based features and vehicle-based online adaptation for predicting EV energy consumption.**

***Index Terms*—Electric vehicles, energy consumption, modeling and prediction, machine learning, field data.**

I. Introduction

A. Motivation & Technical Challenges

Current road transport, heavily relying on fossil fuels, has caused severe public concerns over the energy crisis, air pollution, and global warming. To achieve a sustainable transport system, the mass deployment of electric vehicles (EVs) is imperative and has become an unstoppable trend [1]. According to the International Energy Agency, the global EV stock in the stated policies scenario will expand rapidly from almost 18 million in 2021 to 200 million by 2030, corresponding to an average annual growth of more than 30% [2]. Such electric revolution in the transport sector entails various studies at different levels, ranging from vehicle components (e.g., batteries), individual EVs, and a vehicle fleet, up to traffic networks and their interactions with road infrastructure, power grids, and the environment [3], [4]. Specifically, typical research topics around EVs include but are not limited to battery sizing [5], charging planning [6], driving range prediction [7], routing [8], speed control [9], [10], energy optimization [11], and environmental analysis [12]. To tackle these problems, a common and fundamental task is the development of a reliable and accurate model for EV energy consumption. In addition, such an energy consumption model is a basis for making EV regulations and policies, and for analyzing the supply risks of battery resources.

Accurately and quickly predicting the energy consumption of EVs in completing a given trip is a non-trivial task due to the presence of several technical challenges. First, the energy of an EV is consumed by various resistances (e.g., caused by road friction, gravity, and aerodynamics), inevitable energy losses (e.g., in motors, batteries, and braking systems), and auxiliary vehicle components (e.g., the heating, ventilation, and air conditioning system) while maintaining desired vehicle dynamics and comfort. Furthermore, this process involves a large set of parameters in vehicle design, operation, road topology, traffic states, and the external environment [13], some of which, such as the road conditions, wind speed, and driver behavior, are time-varying and stochastic. Compared to commercial transit buses, private electric cars tend to have complicated and highly volatile trips, and their prediction problem is even more challenging. Last but not least, an instantaneous prediction value is often expected for decision-making and system control, and, in contrast, a trip duration can range from several minutes to hours in which the associated energy consumption is related to vehicle dynamics varying in milliseconds. The multiple timescales involved further complicate the prediction task.

B. Literature Review

Considerable research efforts have been devoted to the modeling of EV energy consumption. The obtained results can generally be categorized into empirical models, physics-based models, and data-driven models.

The simplest empirical models assume constant energy consumption rates in EVs. For example, the electricity consumption has been hypothetically fixed at 1.5 kWh/km in [14] for electric buses in Stockholm, Sweden, whereas it was defined to be 1.2 kWh/km in [15] for mixed bus fleet scheduling. By using the Renault Zoe as a case study, Desreveaux *et al.* demonstrated an important impact of velocity profiles on energy consumption, particularly the maximal velocity, while

The work was supported by Chalmers Foundation and the Swedish Energy Agency under Grant No. P2022-00960. *(Corresponding author: Yicun Huang.)*

Qingbo Zhu, Yicun Huang, and Torsten Wik is with the Department of Electrical Engineering, Chalmers University of Technology, Gothenburg 41296, Sweden (E-mail: qingbo@chalmers.se; yicun@chalmers.se; torsten.wik@chalmers.se).

Chih Feng Lee is with Polestar Performance AB, Gothenburg 41878, Sweden (E-mail: chih.feng.lee@polestar.com).

Peng Liu and Jin Zhang are with the National Engineering Research Center of Electric Vehicles, Beijing Institute of Technology, Beijing 100081, China (E-mail: bitliupeng@bit.edu.cn; bitclzj@163.com).

the maximal acceleration turned out to have a low impact [16]. With this in mind, for improved model accuracy, Wu *et al.* fitted the energy usage as a monotonically increasing polynomial function of the velocity for in-city and freeway driving [17]. Recently, Ji *et al.* developed an analytical model that describes the trip-level energy consumption of the traction and battery thermal management system as a linear logarithmic function of the ambient temperature, curb weight, travel distance, and trip travel time [18]. Similar works can be found in [19] and [20]. Although being useful to analyze and reveal how some parameters affect the energy consumption of a specific EV, or an EV fleet, this class of models ignores many other factors and can suffer from severely degraded performance when being deployed to predict EV energy consumption in a general case.

According to fundamental principles, such as Newton's second law and the law of energy conservation, the dynamics of the mechanical, electrical, and thermal energy states of an EV can be formulated as differential equations, as in [21]–[25]. The obtained physics-based models have been widely used in offline vehicle design [5], simulation-based studies [26], [27], and short-horizon predictive control [9], [10]. However, the application of these models to long-term prediction is challenging due to the need to identify a large number of parameters related to the considered vehicle, driver, road, traffic, and environment, as well as the necessity to update all those time-varying parameters online continuously. To the best of our knowledge, there is currently no well-established physics-based model accurately capturing all the microscopic dynamic behaviors of EVs throughout individual and typical trips. Furthermore, running the physics-based models requires detailed time-series input data concerning the planned trip, such as vehicle and wind velocity profiles, which are not easy to acquire precisely. Even though there is a perfect physics-based model with all its time-varying parameters described by lookup tables or derived by online identification algorithms, and a well-defined trip lasting tens of minutes, it can be computationally expensive to propagate the high-resolution model, e.g., at a sampling time of ten milliseconds, to generate state trajectories for the calculation of accumulated energy consumption. This outrules many applications, such as the planning of trips and charging schedules, where one needs an immediate estimate of energy consumption or even solving an online optimization problem based on the estimated value.

Data-driven modeling approaches using machine learning have recently become very popular in a wide range of research areas, including energy storage, electrified transportation and vehicle technologies [28]–[31], and are good candidates to solve the prediction problem for EV energy consumption. With millions of EVs deployed in the world, it is not technically difficult to collect a statistically sufficient amount of data, though such data may not be readily accessible to many academic research groups. To overcome the data shortage issue, Abdelaty *et al.* used a physics-based model for electric transit buses (ETBs) to generate a large dataset by gradually varying a set of parameters, such as the initial state of charge (SoC), minimum acceleration, average speed, and space between consecutive bus stops, and then developed several machine learning-based models to explain the energy consumption variance [13]. To be more realistic and potentially capture the correlated effects of different vehicle parameters, a few recent studies have made use of real-world vehicle data. For example, Chen *et al.* established a recurrent neural network-based model from time-series ETB data for short-term energy prediction [32]. Towards trip-level predictions based upon field data, relevant models can be found in [33], [34] for ETBs and in [35], [36] for electric cars. The referred works have demonstrated the potential of machine learning-based models for the long-term prediction of EV energy consumption.

C. Contributions of This Work

Inspired by the data-driven models discussed above, this work presents a practical and generic machine learning-based modeling approach for EV energy consumption prediction that not only significantly improves accuracy and robustness, but also provides the prediction uncertainties in real-time. The contributions are systematically achieved by: 1) proposing a new procedure to process and clean real-world EV data, 2) constructing a comprehensive, physics-informed feature pool and extracting the best set of features, 3) applying several powerful machine learning methods to develop prediction models for the consumed energy of an EV fleet with highly diverse trip information, 4) providing the uncertainty range estimation associated with the point prediction, making it useful for corrective actions, decision-making, and safety control purposes, and 5) online adaptation of the selected global models for further improved accuracy and tightened uncertainty range. The proposed machine learning pipeline is illustrated in Fig. 1.

II. Data Description And Processing

A. Dataset

The dataset was collected by the National Monitoring and Management Platform for New Energy Vehicles in China from 55 battery electric taxis of the same brand and model. Equipped with lithium nickel cobalt manganese oxide (NCM) batteries having 30.4 kWh nominal capacity, these taxis were designed to have a driving range of up to 200 km and a maximum speed of 125 km/h. More specifications about them can be found in [35]. The states of vehicle operation (e.g., mileage and speed), batteries, motors, motor controllers, the braking system, fault alarms, and insulation resistance, as well as the location information, were monitored in real-time. The corresponding data were sent to the platform via wireless communication at a nominal frequency of 1 Hz. The detailed data items, formats, and communication protocols follow the standard given in [37]. The selected data reflect vehicles running in Beijing, with the earliest data points from March 2017 and the latest from December 2018.

The obtained time-series data for each vehicle were segmented into different driving trips, where the trips end whenever a stop or idling state is longer than three minutes. In practice, these trips could be terminated due to parking or charging. When there was no data uploading, embodied as data missing, or a series of zeros for more than three minutes,

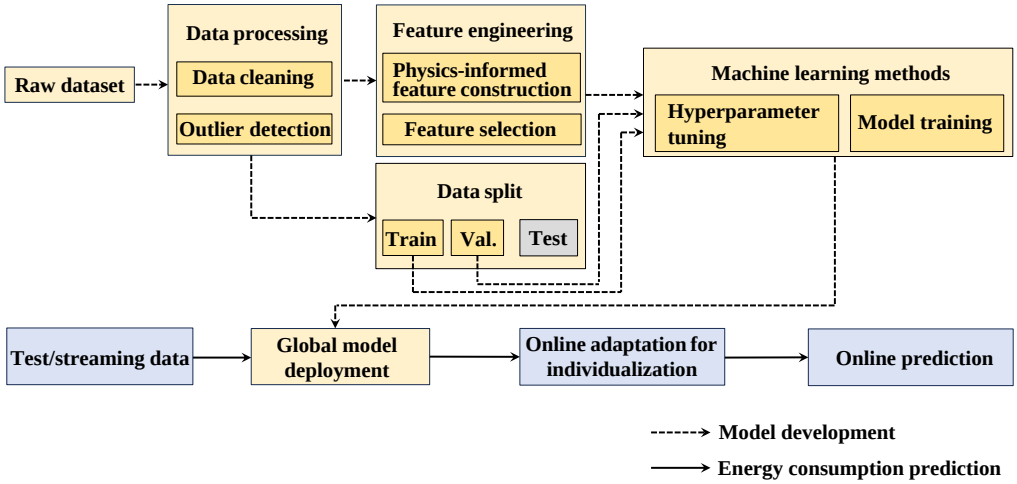

Fig. 1: Pipeline to develop data-driven algorithms for energy consumption prediction.

we also considered it as a trip completion. The data samples between every two consecutive trips were ignored as the corresponding energy consumption was negligibly small. Without energy consumption information from the vehicle cabin, e.g., for heating, ventilation, and air conditioning (HVAC), the energy output from the motors has been considered as the system output of interest, y, and was calculated by the time integral of the product of the measured current and voltage over the motor.

The measured GPS data from vehicles were input into Google Earth to generate road elevation data allowing calculation of road grade profiles. According to the recorded time and position, the external environment measurements, including ambient temperature, wind speed and direction, dewpoint temperature, and humidity, were taken from the weather website (https://www.xihe-energy.com) at a sampling time of 30 minutes.

All the trips were labeled by dates, and when the daily driving ranges became outside of $[1, 600]$ km, the corresponding trips were dropped. When the daily driving ranges are less than 1 km, the included trips are very short, rendering the energy consumption prediction unnecessary. On the other hand, it is unusual for these taxis to drive 600 km in a day as it means three full charges. As a result, a total of 91,932 trips were extracted from the raw vehicle data. Fig. 2 exemplifies the time-series velocity, acceleration, and elevation within two trips and illustrates the distribution of their trip-level average values over all the trips. It can be seen that the driving profiles vary largely within a specific trip and among different trips.

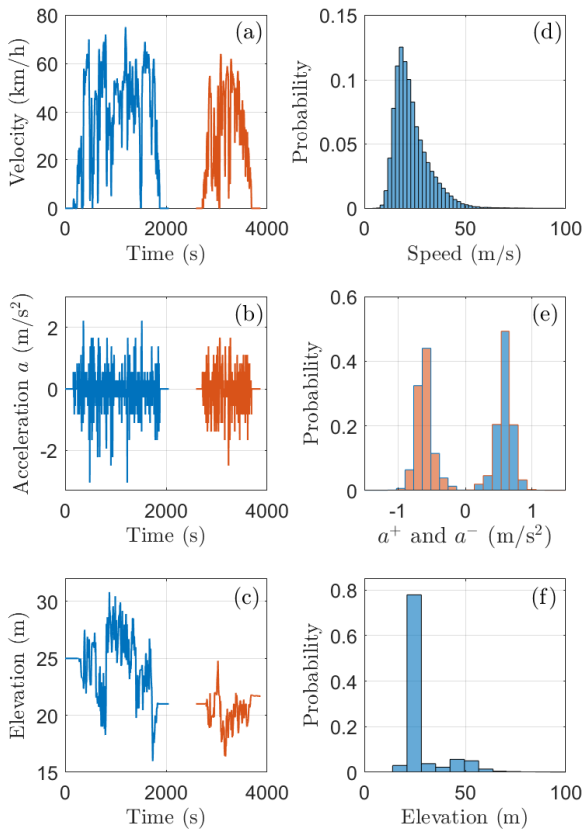

Fig. 2: Data measured from electric taxis. (a)-(c) show the velocity, acceleration, and elevation profiles, respectively, of two continuous trips of a vehicle. (d)-(f) illustrate the histogram trip-level average velocity, acceleration, and elevation, respectively, over all the trips, where both the positive acceleration, a^+, and the negative acceleration, a^-, are considered.

B. Data Processing

The dataset described in Section II-A was transmitted wirelessly from the running taxis to the data platform. However, wireless transmission is susceptible to interference and can be affected by long distances, physical obstructions, channel disturbance, and weather conditions. In addition, digital-to-analog conversion, sensor noise, and differentiation of measurements may also cause problems. Under such circumstances, our dataset should have inherently suffered from issues, such as measurement noise, data latency, loss, or mismatch. Given that data quality is critical for machine learning, the existing issues will inevitably weaken and even undermine the accuracy and

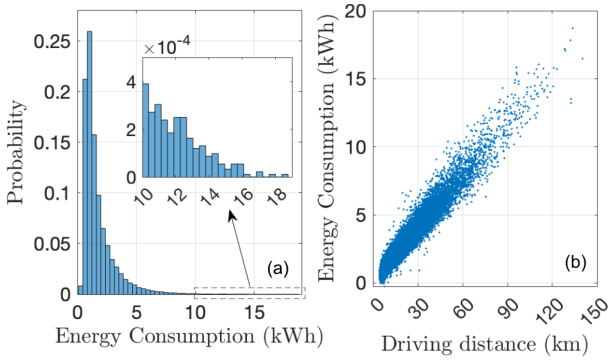

Fig. 3: Illustration of raw data samples. (a) Probability of energy consumption over all the trips. (b) Total energy consumption of each trip versus the corresponding driving distance.

reliability of data-driven models for predicting vehicle energy consumption. Hence, it is necessary to process and clean the data. To do so, we use knowledge of vehicle usage and kinetics as well as statistical properties to phase out potential issues.

1) Data Cleaning. For any given trip $i \in \{1, 2, \cdots, \bar{N}\}$, where $\bar{N}$ is the number of all trips, we identify and quantify the data loss by comparing the number of existing time-series data samples, denoted by M_i, to its expected value Σ_i. The data loss rate, $\rho_{\text{loss},i}$, is defined as

$$\rho_{\text{loss},i} = (\Sigma_i - M_i)/\Sigma_i. \tag{1}$$

With the frequency of 1 Hz in collecting data, it is common that exists $\rho_{\text{loss},i} > 0$. Analogously, the data mismatch rate, $\rho_{\text{mismatch},i}$, is calculated by

$$\rho_{\text{mismatch},i} = (M_i - M_{\text{mismatch},i})/M_i, \tag{2}$$

where $M_{\text{mismatch},i}$ is the number of expected data samples and it can be exemplified as the situation where the motor current is zero while the vehicle speed is nonzero.

2) Outlier Detection. Some outliers in the obtained dataset can be detected from the labeled output while others can be isolated based on the trip-level features x that impact the system output. As illustrated in Fig. 3(a), some trips have consumed unusually more energy than others while a small number of trips are on the other side of the spectrum. From Fig. 3(b), it can be observed that the trip-level average energy consumption y_i tends to be linearly related to the driving distance d_i. In the bottom-left corner of the sub-figure, some trips are featured with over 10 km driving distance whereas the corresponding energy consumption is around zero. To systematically deal with these outliers, we combine the concepts of studentized residuals and leverage [38] to distinguish extreme output values in $\{y_1, \cdots, y_{\bar{N}}\}$ and extreme feature values in $\{d_1, \cdots, d_{\bar{N}}\}$.

Suppose $y_i = d_i\beta + \epsilon$ for the relationship between the energy consumption y_i and driving distance d_i, where β is a scalar coefficient and ϵ is a parameter vector, representing the slope and bias of the linear regression model, respectively. Then, according to the analytical solution to the linear least squares problem, the optimal value can be obtained as $[\beta, \epsilon]^T = (D^T D)^{-1} D^T Y$, where $Y = [y_1, \cdots, y_{\bar{N}}]^T$ and $D = [d_1, 1; \cdots; d_{\bar{N}}, 1]$. By defining D's pseudoinverse as $D^\dagger$, namely $D^\dagger = (D^T D)^{-1} D^T$, the estimated value of Y is given by

$$\hat{Y} = \begin{bmatrix} D^\dagger_{11} & D^\dagger_{12} & \cdots & D^\dagger_{1\bar{N}} \\ D^\dagger_{21} & D^\dagger_{22} & \cdots & D^\dagger_{2\bar{N}} \\ \vdots & \vdots & \ddots & \vdots \\ D^\dagger_{\bar{N}1} & D^\dagger_{\bar{N}2} & \cdots & D^\dagger_{\bar{N}\bar{N}} \end{bmatrix} Y, \tag{3}$$

where $D^\dagger_{ii}$ is the leverage value and it indicates the distance between a certain driving distance d_i and the average value of d_i for all the $\bar{N}$ trips.

According to its definition, the studentized residual for trip i, denoted by r_i, is given by [38]

$$r_i = \frac{y_i - \hat{y}_i}{\sqrt{\sigma(y_1, \cdots, y_{\bar{N}}) \cdot (1 - D^\dagger_{ii})}}, \tag{4}$$

where $\hat{y}_i$ is derived from (3), $y_i - \hat{y}_i$ represents the ordinary residual for trip i, and the function $\sigma(\cdot)$ is the standard deviation of y_i in all the $\bar{N}$ trips.

III. Overview of Physics-based Modeling

In general, the energy consumption of a vehicle is to overcome several types of driving resistance and to support auxiliary systems, e.g., HVAC. At the same time, it will be affected by regenerative braking and energy efficiencies in the powertrain system and its components. By only considering energy flow from the vehicle motors, the energy consumption of an electric vehicle, $\hat{y}$, can be calculated by

$$\hat{y} = F_r d/\eta_r + \eta_b E_{\text{brake}}, \tag{5}$$

where F_r represents the propulsion force, E_{brake} is the regenerative braking energy, and η_r and η_b denote the corresponding energy efficiencies. According to Newton's second law of motion, the propulsion force applied to vehicles can be expressed as [22]

$$\begin{aligned} F_r = {} & mgf\cos(\theta) + \frac{C_D A (V - V_{\text{air}})^2}{21.15} \\ & + mg\sin(\theta) + \delta ma, \end{aligned} \tag{6}$$

where the four terms on the right-hand side of (6) represent the rolling resistance, air resistance, climb resistance, and acceleration resistance. g, δ, and C_D denote the gravitational acceleration, the transfer coefficient from the revolving mass to a linear mass, and the drag coefficient, respectively, and these three parameters are generally constant during vehicle movement. m, A, and f are the vehicle mass, equivalent cross-sectional area, and tire rolling resistance coefficient. While m can vary among different trips for a taxi, f and A are heavily influenced by road conditions and the ambient environment. θ, V, and V_{air} are the road grade, vehicle velocity, and wind velocity, which are variables in a trip.

If all the model parameters in (6) are known *a priori* and all the variables can be measured accurately, the instantaneous propulsion force can be calculated directly at each time step. However, as noted in the introduction, these parameters and a set of energy efficiencies for a vehicle system can be affected

by many complicated factors, and it is very expensive and difficult to quantify them accurately, particularly considering the wide range of uncertainties and stochasticity during vehicle usage.

IV. Data-driven Model Development

Fully recognizing the complexities involved in precise parameterization and long-term simulation of physical models, this study adopts a data-driven approach to efficiently forecast the trip-level energy consumption of EVs. This approach incorporates a set of features carefully constructed from the physics-based model described in Section III.

A. Physics-informed Feature Construction and Engineering

The first step in establishing a machine learning (ML) model is to extract elements for feature construction. All these elements are taken directly or are inspired by the physics-based model (6). As such, all essential physical insights into energy consumption can be systematically incorporated into the ML-based prediction model. As shown in the first three columns of Table I, these elements can be categorized into four classes, i.e., trip intrinsic attributes, road characteristics, vehicle states, and ambient environments. Note that in addition to the instantaneous acceleration, the positive and negative values of acceleration are considered to better reflect the vehicle states on the trip level. The relative wind velocity V_w, defined as $V - V_{\text{air}}$, is also considered as part of the ambient environment.

With these physics-informed elements, a two-step procedure is used to construct a comprehensive feature pool. First, the time-series data of each of the considered elements over a given trip is transformed into a form of histogram. Then, a variety of statistical properties of the histogram can be extracted, including the mean, variance, 0.95 quantile, and 0.05 quantile, which represent the characteristics of central tendency, dispersion, and extreme situations of each driving trip, respectively. The obtained library of elements and corresponding constructed features is listed in Table I. Note that in the absence of measured data, our feature pool does not explicitly incorporate locally distributed traffic information, such as traffic density and congestion levels. However, we anticipate that the selected features related to vehicle velocity and acceleration implicitly capture the effects of varying traffic conditions on trip-based energy consumption.

This employed feature construction strategy compresses hundreds or thousands of time-series data samples in a trip into a small number of features, corresponding to each physical element. The strategy reduces the scale of the input data by several orders of magnitude, resulting in significantly decreased memory resources to store the data and computational cost to train ML models. In addition, it enables efficient predictions during the online implementation. Such a strategy is imperative when the raw data are stored originally and locally as histograms within the vehicle. A similar strategy was used in [39] to compress vehicle field data for predicting the aging trajectory of lithium-ion batteries.

With the constructed feature pool, feature engineering is conducted to select a set of most relevant and independent features for the development of ML models. To achieve this, Spearman correlation analysis is first conducted to assess the correlation between any feature x and the system output y. The Spearman's rank correlation coefficient ρ_s that measures the strength and direction of the monotonic relationship between x and y can be calculated as [40]

$$r_i = R_{x_i} - R_{y_i}, \tag{7}$$

$$\rho_s = 1 - \frac{6\Sigma_{i=1}^{N_{\text{train}}} r_i^2}{N_{\text{train}}(N_{\text{train}}^2 - 1)}, \tag{8}$$

where i is the index of the trip-based data samples, N_{train} represents the number of training samples, and R_{x_i} signifies the rank of x_i after sorting all training samples for the considered feature in ascending order. By setting a lower threshold for the Spearman's rank correlation coefficient, i.e., $\rho_{s,\min}$, any features with a score less than $\rho_{s,\min}$ will be discarded from the feature pool. Following the analysis for the correlation between any feature and the system output, Pearson correlation analysis [40] is applied to quantify the correlation between any two features within the remaining pool. For each feature pair, when the Pearson correlation coefficient ρ_p is greater than a specified upper threshold $\rho_{p,\max}$, the feature with a lower value of ρ_s is abandoned to avoid multicollinearity among features.

B. ML-based Prediction Models

Within the realm of supervised machine learning, the prediction of trip-based EV energy consumption is framed as a regression problem in terms of the selected features and the consumed energy y. The target is to develop reliable and accurate ML models that provide trip-wise point predictions and the associated uncertainty range, where the latter aims to make the prediction results interpretable. Four regression algorithms, specifically the quantile regression (QR), quantile regression neural network (QRNN), quantile extreme gradient boosting regression (QEGBR), and quantile regression forests (QRF), are utilized in the offline pathway of Fig. 1 to develop novel prediction models for y. Note that none of these quantile-based algorithms relies on the assumption of any specific distribution of the system output, unlike other probabilistic models, such as Gaussian process regression.

1) QR: QR is a robust learning algorithm for estimating the conditional quantiles of the target, y, from data, as opposed to solely focusing on the median. From a physical perspective, it divides the training dataset into two segments based on the value of quantile hyperparameters. The QR's check function, $\rho_\tau(e_i, \tau)$, can be written as [41]

$$\rho_\tau(e_i, \tau) = \begin{cases} -(1-\tau)e_i & \text{if } e_i < 0 \\ \tau e_i & \text{if } e_i \geq 0, \end{cases} \tag{9}$$

where the parameter $\tau \in (0, 1)$ represents the quantile of y, and the discrepancy between y_i and its predicted value $\hat{y}_i$ is defined as $e_i = y_i - \hat{y}_i$ for the i-th trip. If $\tau = 0.5$, the goal is to fit a straight line that divides the dataset into two equal

TABLE I: Elements for feature construction and the resulting feature pool

Element classification	Elements	Description	Features
Trip intrinsic attributes	d	Driving distance of a trip	d
	t_d	Driving time of a trip	t_d
Road characteristics	E	Elevation of the road	mean, variance, 0.95 quantile, 0.05 quantile
	$G^{\cos}$	Cosine value of road grade	mean, variance, 0.95 quantile, 0.05 quantile
	$G^{\tan}$	Tangent value of road grade	mean, variance, 0.95 quantile, 0.05 quantile
Vehicle states	V	Vehicle velocity	mean, variance, 0.95 quantile, 0.05 quantile
	V^2	Square of vehicle velocity	mean, variance, 0.95 quantile, 0.05 quantile
	V^3	Cube of vehicle velocity	mean, variance, 0.95 quantile, 0.05 quantile
	a	Acceleration of vehicle	variance, 0.95 quantile, 0.05 quantile
	a^+	Positive vehicle acceleration	mean
	a^-	Negative vehicle acceleration	mean
Ambient environments	V_w	Relative wind velocity	mean, variance, 0.95 quantile, 0.05 quantile
	V_w^2	Square of relative wind velocity	mean, variance, 0.95 quantile, 0.05 quantile
	T_a	Ambient temperature	mean
	T_d	Dewpoint temperature	mean
	H	Humidity	mean
	P	Precipitation	mean

parts, which is equivalent to using the absolute loss (AL), $\mathcal{L}_{AL}(y_i, \hat{y}_i) = \sum_{i=1}^{N_{\text{train}}} |y_i - \hat{y}_i|$, as the loss function in linear regression. The determination of the upper and lower bounds for a specified prediction interval can be achieved by setting the values of τ in (9).

2) QRNN: Neural networks (NNs), drawing inspiration from the human brain, are computational models composed of interconnected nodes structured into layers. These nodes incorporate weighted connections and activation functions, enabling them to process data through feedforward computations for predictive tasks. The training process, known as back-propagation, refines these networks that often include multiple hidden layers to facilitate deep learning. Deep neural networks (DNNs) are a type of NNs characterized by having multiple hidden layers, providing them with the ability to learn intricate representations, attain high model performance, and effectively process extensive datasets. In DNNs for regression problems, the most commonly used loss functions are the squared loss (SL) and AL, but they are restricted to making point predictions. According to [42], by integrating the QR algorithm into a DNN structure, one can obtain both the point prediction $\hat{y}$ and the uncertainty range estimation associated with $\hat{y}$. In this work, we incorporate the QR check function into the loss function of QRNN, namely $\mathcal{L}(y_i, \hat{y}_i) = \sum_{i=1}^{N_{\text{train}}} \rho_\tau(e_i, \tau)$.

3) QEGBR: Extreme gradient boosting (XGBoost) is a scalable end-to-end ML algorithm that leverages gradient tree boosting to create ensemble models for predictions and classifications [43]. Unlike linear regression and NNs, which offer flexibility in choosing loss functions that can be first- or second-order differentiable, the loss function of XGBoost needs to be second-order differentiable as Newton's method is required for the optimization [44]. Commonly, the log-cosh loss function is applied in XGBoost with the following form:

$$\rho_{LC}(y_i, \hat{y}_i) = \log(\cosh(\hat{y}_i - y_i)). \tag{10}$$

Similar to classic DNNs, the XGBoost can provide point prediction but not the uncertainty range. To have both the point and uncertainty range predictions, one would naturally expect some appropriate combinations of XGBoost and QR. Given that QR's loss function is not second-order differentiable at the origin, a second-order differentiable function can be introduced to create a smooth approximation of the QR loss function, allowing for a smooth transition at the origin [45]. With this in mind, we replace $\hat{y}_i - y_i$ in (10) by the quantile check function $\rho_\tau(\hat{y}_i - y_i, \tau)$ defined in (9). The obtained algorithm integrates XGBoost and the new quantile loss function and is consequently termed QEGBR.

4) QRF: Different from the previous three parametric quantile regression methods, which predict the target value by minimizing their respective loss functions, random forest-based algorithms are non-parametric tree-based approaches without the process of optimizing parameters. QRF is a generalization of the original random forest (RF) [46]. When constructing the forest, both QRF and RF utilize decision trees, employ bootstrapping to generate distinct subsets of data, and make random selections for nodes and splitting points. In RF, the predicted value is the conditional mean, which is approximated by averaging the predictions from all the trees in the forest. Therefore, the only information needed in RF is the mean of the observations that fall into each node across all trees. Different from RF, QRF retains all the values of all observations in all nodes, not just their mean, and then uses this information to assess the target conditional distributions under different quantiles, thereby generating predictions for the system output and the associated uncertainty.

C. Online Model Adaptation for Customized Prediction

The global models in Section IV-B are trained and validated on historical vehicle data. When we apply the resulting models to predict vehicle energy consumption, they are blind to the unique characteristics of new vehicles whose driving situations may deviate largely from those in the training set. The predictions are essentially generated from an open-loop simulation based on the global models. The historical driving data of a targeted vehicle during real-world usage shall contain valuable information for understanding and learning the characteristics of its future energy consumption. Taking this individualized information into consideration as feedback, online adaptive models can be developed to potentially improve the prediction performance, particularly for vehicles that have not been seen

during the training process. To test this concept for EV fleets, we for the first time develop online adaptive models for EV energy consumption based on QRNN and QEGBR, where model adaptations are made in real-time based on the latest trip the targeted vehicle has completed.

1) Online Adaptive QRNN: With continuous usage of the targeted vehicle, new data samples will be available and can be used for individualized model development. The QRNN often consists of many layers and neurons to learn complex input-output relationships.

On one hand, if training the entire QRNN model at each time step k only against the newly arrived data sample, one can expect serious over-fitting. On the other hand, by adding the newly arrived data to the training set for model re-training, the required time can be very long, hindering online model adaptation. In addition, the result of model re-training will still be dominated by the offline available dataset. To enhance the impact of new data and facilitate efficient online learning, we adopt a learning-without-forgetting approach proposed in [47]. The key idea is that while the overall structure and the values of most parameters of the global model are preserved, the parameters of the hidden layer closest to the output layer, denoted Θ, are updated as the new data sample arrives. While various online parameter estimation methods can be applicable, for demonstration purpose, we employ the stochastic gradient descent to estimate Θ_k recursively according to

$$\Theta_{k+1} = \Theta_k - \alpha \nabla \mathcal{L}(\Theta_k), \tag{11}$$

where $k+1$ means the trip next after trip k, α represents the learning rate, and $\nabla \mathcal{L}(\Theta_k)$ is the gradient (vector) of the loss function of QRNN with respect to Θ_k.

2) Online Adaptive QEGBR: XGBoost can be implemented through a mature and well-encapsulated toolbox, which limits modifications to the global model trained offline. The core of the QEGBR algorithm involves adding trees and repeatedly performing feature splits to grow a tree, where a new function is learned each time, and a tree is added to fit the residual from the previous prediction. To have the benefits of both offline and online learning, we propose the online adaptive QEGBR algorithm. Specifically, with the arrival of each new training data from a targeted vehicle, we add a new tree in its modeling to reduce the residual, thereby enabling individualized modeling for this specific vehicle in real-time. Differing from the online adaptive QRNN, the online adaptive QEGBR thus alters the structure, rather than the parameters, of its corresponding global model.

Note that during the online phase, both the above two adaptation algorithms will preserve the major model information from the previous learning step to reduce the risk of overfitting, robustness issues, and large modeling errors.

V. Results And Discussion

Four evaluation metrics are applied to evaluate the prediction accuracy and uncertainty estimation performance. Two of them are used to analyze the prediction accuracy, namely the root mean squared error (RMSE) and the percentage mean absolute error (PMAE) defined as

$$RMSE = \sqrt{\frac{1}{N}\sum_{i=1}^{N}(y_i - \hat{y_i})^2}, \tag{12}$$

$$PMAE = \frac{\frac{1}{N}\sum_{i=1}^{N}|y_i - \hat{y_i}|}{\frac{1}{N}\sum_{i=1}^{N}|y_i|} \times 100\%, \tag{13}$$

where N is the number of data samples in the testing set. The other two evaluation standards for assessing prediction intervals at the same probability level are the coverage probability (CP) and average width (AW) of the prediction interval, defined as

$$PI_{\text{CP}} = \frac{1}{N}\sum_{i=1}^{N} C_i, \text{where } C_i = \begin{cases} 1 & y_i \in [\underline{y}_i, \overline{y}_i] \\ 0 & y_i \notin [\underline{y}_i, \overline{y}_i] \end{cases} \tag{14}$$

$$PI_{\text{AW}} = \frac{1}{N}\sum_{i=1}^{N}(\overline{y}_i - \underline{y}_i), \tag{15}$$

where $\underline{y}_i$ and $\overline{y}_i$ represent the predicted lower and upper bounds, respectively, for a certain prediction interval.

A. Implementation Specification

For data processing in Section II-B, to balance the degree of removing the detected issues and the number of data samples in model development, we set the tolerable thresholds for $\rho_{\text{loss},i}$ and $\rho_{\text{mismatch},i}$ to 10% and 30%, respectively. Any trips in the dataset that do not satisfy the conditions will be removed. We flag trip-level samples as outliers when $D_{ii}^{\dagger}$ exceeds $6/\bar{N}$ or the absolute value of r_i is larger than 3.

We use Monte Carlo cross-validation to evaluate the accuracy, efficiency, and robustness of the developed ML models. From the processed dataset, 45 vehicles are randomly selected and used for model training, while the data from the remaining 10 vehicles serve as the test set. This process of random data splitting is iterated 20 times to mitigate sample bias. Subsequently, the average results of these iterations are computed to provide a robust assessment of model performance. For feature engineering in Section IV-A, we set $\rho_{s,\min} = 0.05$, and $\rho_{p,\max} = 0.8$.

For all the ML algorithms described in Section IV-B, the quantile values, τ, in their corresponding loss functions are set as 0.5 for generating point predictions. The quantile values are set to be 0.025 and 0.975 to obtain the lower and upper bounds, of a 95% prediction interval, respectively.

B. Results of Data Processing

The results of data processing, including data cleaning and outlier detection conducted in Section II-A, are partially depicted. For brevity, only the data on trip-based energy consumption and its correlation with driving distances are presented in Fig. 4.

Compared with the raw data samples displayed in Fig. 3, the shapes of these two histogram plots are highly similar, both exhibiting a distinct right skewness. This means most trips had low energy consumption. However, the distribution of the

cleaned dataset has a shorter and lighter tail than that of the raw dataset. Specifically, the trips with energy consumption of more than 15 kWh, which is about 50% of the maximum energy stored in the battery system at the beginning of its life, are largely reduced. The removed data samples particularly include "skeptical trips" that consumed high energy within short driving distances. After the data processing, the linearity between driving distances and energy consumption becomes more pronounced, and correspondingly, the variation of energy consumption generally becomes smaller for a given driving distance.

In total, 91,932 driving trips are extracted from the original time-series data. According to the tolerable thresholds of data loss and mismatch in each trip specified in Section V-A, 53.88% of the data samples are removed. After the data cleaning, 816 data samples belong to the defined outliers, corresponding to 0.8876% of the raw data. Overall, 41,585 samples are retained for the training and testing of ML models.

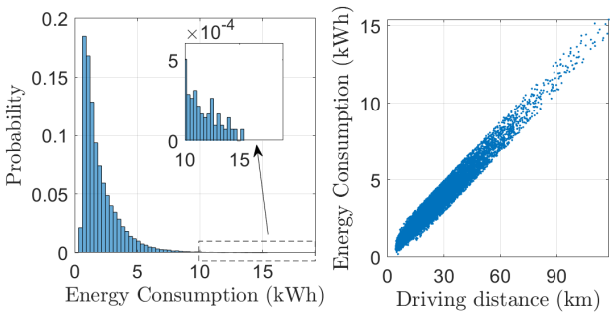

Fig. 4: Illustration of the trip-based energy consumption data resulting from data cleaning and outlier detection.

C. Results of Feature Engineering

This subsection presents results of feature engineering performed in Section IV-A using $\rho_{s,\min}$ and $\rho_{p,\max}$ specified in Section V-A. Table II lists the 17 selected features and their coefficients of Spearman correlation with the output y, i.e., the trip-based energy consumption. For Pearson correlation between each two features, the coefficients are also derived, and Fig. 5. depicts the scores for the features applied in the ML models.

The driving distance d is found as the most relevant feature to predict y, having a Spearman correlation coefficient as high as 0.98. However, several other features also correlate strongly with y, such as the driving time. However, these features are heavily dependent on d according to the Pearson correlation analysis and were therefore excluded to mitigate multicollinearity. In general, features related to vehicle states are more relevant to y than those features associated with the ambient environment. Specifically, the 95th quantile of the vehicle velocity carries more weight than the average velocity, and the variance of acceleration takes precedence over all other acceleration-related features. It is noteworthy that the impact of both the variance of the relative wind velocity and the elevation on y is substantial, which is an underexplored aspect in the existing literature.

TABLE II: The selected features and their Spearman correlation coefficients

Feature	Description	Coefficient
d	Driving distance	0.9831
$V_{w,\text{var}}$	Variance of relative wind velocity	0.4126
E_{var}	Variance of elevation	0.3928
V_{95}	95th quantile of vehicle velocity	0.2945
V_{ave}	Average of vehicle velocity	0.2422
a_{var}	Variance of acceleration	0.2126
E_{95}	95th quantile of of elevation	0.1871
$G^{\cos}_{\text{var}}$	Variance of $G^{\cos}$	0.1576
$G^{\cos}_{95}$	95th quantile of $G^{\cos}$	0.1399
T_d	Average of dewpoint temperature	0.1313
P	Mean precipitation	-0.0944
H	Mean humidity	0.0880
$V_{w,5}$	5th quantile of relative wind velocity	-0.0879
$G^{\tan}_{5}$	5th quantile of $G^{\tan}$	0.0752
V_5	5th quantile of vehicle velocity	-0.0665
$G^{\tan}_{95}$	95th quantile of $G^{\tan}$	-0.0618
$G^{\tan}_{\text{var}}$	Variance of $G^{\tan}$	0.0586

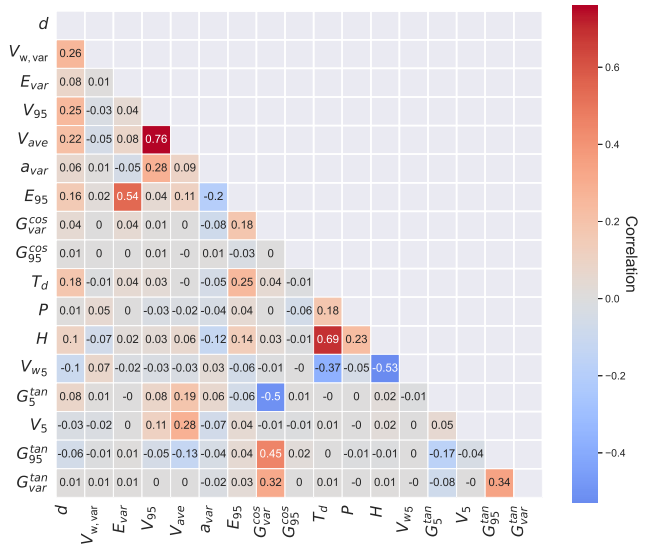

Fig. 5: Pearson correlation heatmap of the selected features for the processed dataset.

D. Results of the global ML models

1) Prediction Accuracy: By using the ML-based prediction models developed in Section IV-B, we can continuously predict EV energy consumption in each trip. With the data split defined in Section V-A and the obtained hyperparameters in Table III, the overall prediction results for all data samples in the test set are summarized in Tables V–IV.

Although the task is challenging, it can be observed that the best model, i.e., QRNN, can accurately predict EV energy consumption. Specifically, after cleaning the data and removing the outliers, the QRNN model can deliver predictions with a PMAE of 6.3%. In addition to QRNN, QEGBR can also effectively learn the characteristics of energy consumption from the diverse field data and make reliable predictions for any given input that has not been seen during training. These results verify the effectiveness of the developed energy consumption models as well as the constructed and selected

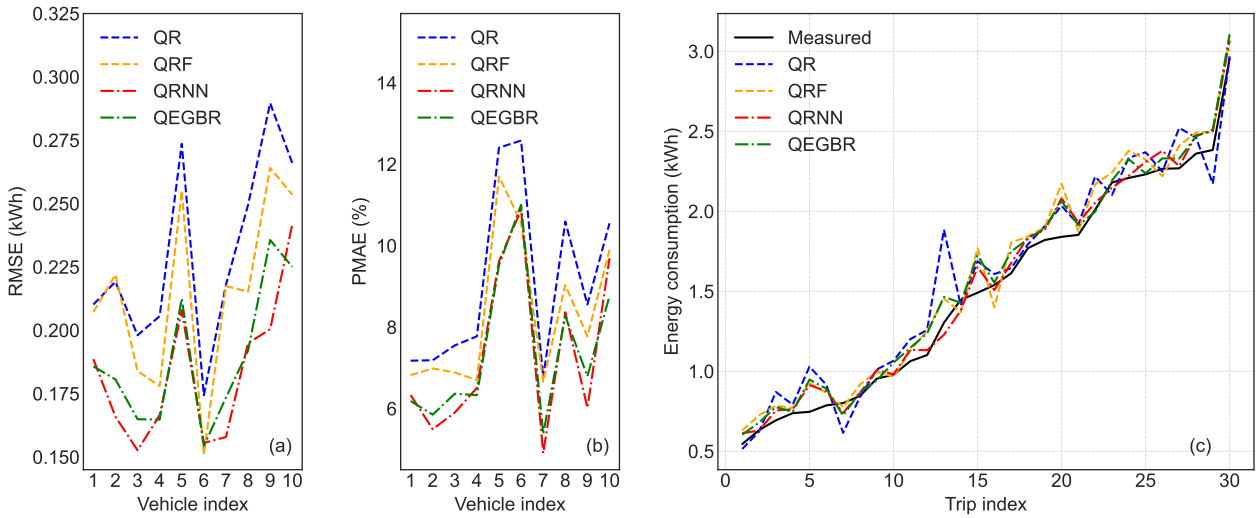

Fig. 6: Prediction results of the four global models for individual vehicles. (a) and (b) show the RMSE and PMAE values. (c) exemplifies the predicted energy consumption in 30 trips from a randomly selected vehicle in the test set.

TABLE III: Hyperparameter values for the applied ML algorithms

QR	—
QRNN	Hidden unit numbers: 256, 64, 32, 32, 8 L2 regularization: 0.0005 Learning rate: 0.00001
QEGBR	Learning rate: 0.01 Total number of iterations: 8000 Early stopping rounds: 10
QRF	Maximum features: 17 Maximum tree depth: 20 Minimum sample split: 10 Minimum sample leaf: 2

physics-informed features underlying each model.

To evaluate the efficacy of our newly developed global models for energy prediction, as well as their underlying feature set (i.e., those in Table II and labeled here as Set 4), we compare the obtained results with those achieved in three benchmarks using different feature sets. The first benchmark has a feature set (i.e., Set 1) only incorporating driving distance. The second benchmark adopts a more complex feature set derived in the state-of-the-art literature [35], which includes driving range, driving time, average velocity, 95% quantile of acceleration, 5% quantile of acceleration, and average temperature, and six categorical variables representing traffic conditions during rush and non-rush hours across various time frames and days. The third benchmark employs the proposed feature engineering but only takes the ten features with the highest correlation coefficients from Table II, forming Set 3. To ensure a fair comparison, all four machine learning (ML) models were implemented and fine-tuned across each benchmark. The results demonstrate a clear advantage of using our comprehensive feature set (Set 4). Notably, our QRNN model achieves a reduction in prediction error of 11.9% compared to the best-performing benchmark and 19.6% relative to the state-of-the-art benchmark.

To assess the impact of data processing on prediction accuracy, we conducted a comparative analysis of results using the raw dataset and two processed datasets. Our findings indicate significant improvements in prediction accuracy after data cleaning and outlier removal, as evidenced by reductions in both the RMSE and PMAE. By using QRNN as an example, without the proposed data processing techniques, the PMAE can become 41% larger, and the RMSE will increase by 29%. Analysis of the results presented in the last two columns of Table V underscores that in addition to addressing data loss and mismatch issues, it is crucial to remove outliers.

Upon detailed examination of the results, it is observed that for the two less accurate models, i.e., QR and QRF, the RMSE values exhibit a marginal increase after the data cleaning, a phenomenon that initially appears counter-intuitive. It is found that the prediction errors from QR and QRF models tend to escalate for longer trips. The data cleaning process primarily removes data samples pertaining to shorter trips, which results in an increase in the average trip distance within the cleaned dataset. Consequently, this leads to slightly increased RMSE values, specifically 0.274 for the QR model and 0.2506 for the QRF model. This observation further corroborates the significance of outlier removal from the dataset.

By using the processed dataset, the prediction results for individual vehicles in the test set are illustrated in Fig. 6. QRNN and QEGBR generally outperform the other two models for individual vehicles and trips, consistent with the results obtained above. It can also be seen that the prediction errors do not appreciably increase with energy consumption (Fig. 6c), showing the stability and robustness of the developed models. This implies that for trips with higher energy consumption, the relative errors tend to be smaller. In Fig. 6a–b, the trajectories of the four ML models have a similar variation trend. This conveys that in addition to the ML algorithms, the prediction results are also influenced by other factors, such as the data quality in terms of resolution and level of detail. It may be

TABLE IV: Effects of different feature sets and online learning on prediction accuracy

Model	Error type	Global models with different feature sets				Online adaptive models
		Set 1	Set 2	Set 3	Set 4	Set 4
QR	RMSE	0.2891	0.2365	0.2343	0.2263	
	PMAE	10.37%	8.29%	8.17%	7.90%	
QRF	RMSE	0.2868	0.2232	0.2266	0.2132	
	PMAE	10.26%	7.88%	7.92%	7.31%	
QRNN	RMSE	0.2870	0.2193	0.2129	0.1788	0.1456
	PMAE	10.30%	7.84%	7.23%	6.30%	5.04%
QEGBR	RMSE	0.2875	0.2120	0.2012	0.1861	0.1604
	PMAE	10.28%	7.50%	6.97%	6.47%	5.56%

TABLE V: Prediction errors of the developed models using different datasets

Model	Error type	Raw data	Data with outliers	Fully processed data
QR	RMSE	0.2694	0.2740	0.2263
	PMAE	10.23%	8.43%	7.90%
QRF	RMSE	0.2482	0.2506	0.2132
	PMAE	9.54%	7.70%	7.31%
QRNN	RMSE	0.2311	0.2262	0.1788
	PMAE	8.88%	7.00%	6.30%
QEGBR	RMSE	0.2247	0.2128	0.1861
	PMAE	8.84%	6.74%	6.47%

noticed that for test vehicle No. 6, the predictions have a low RMSE but a high PMAE. This is because we have used the average energy consumption of all its trips, and shorter distances traveled by this vehicle result in a larger PMAE value.

2) Uncertainty Estimation: To make the predictions interpretable for decision-making of EV charging and energy usage, four quantile-based ML algorithms have been used in the prediction model development allowing the uncertainty associated with each prediction to be estimated at the same time. To the best of our knowledge, this has not previously been conducted in the literature of data-driven EV energy prediction. The coverage probability and average width of prediction intervals, i.e., PI_{CP} and PI_{AW}, are used to quantify the performance of uncertainty estimation, with the results presented in Table VI and Fig. 8. Without doubt, one would desire prediction intervals to always cover the ground truth (i.e., high PI_{CP}) and to be as narrow as possible (namely low PI_{AW}). Within a 95% confidence interval, the ideal PI_{CP} for models evaluated on the test dataset is 0.95, though the actual values of PI_{CP} may vary with the data distribution of the test dataset and model structures.

From the numerical and graphical results, it can be seen that the prediction intervals generated by QR, QRF, and QRNN are able to cover the measured trip-level energy consumption on most occasions. While QR gives the highest PI_{CP}, QEGBR results in lowest PI_{AW} thanks to the use of the synthetic quantile loss function, i.e., $\rho_{LC}(y_i, \hat{y}_i) = \log(\cosh(\rho_\tau(\hat{y_i} - y_i, \tau))$ as described in Section IV-B3. QRNN is capable of best balancing PI_{CP} and PI_{AW}, and can consequently serve as the most suitable candidate for uncertainty estimation. By leveraging QRNN's prediction interval bounds, i.e., $\underline{y}_i$ and $\overline{y}_i$ generated for each trip i, it is possible to establish suitable constraints and safety margins for various decision actions.

3) Computational efficiency: In addition to performance for point prediction and uncertainty estimation, the computational efficiency of ML models is crucial for real-time implementations. With this consideration, we investigate the computational time required by all the developed models. It is found that the most accurate global model, namely the QRNN, requires only 15 microseconds on average to predict the energy consumption for individual trips. This time is significantly less than the trip duration, rendering it negligible.

E. Results of Online Adaptive Models

The best global models, i.e., QRNN and QEGBR, have been adapted online, with the results demonstrated in Table V and Fig. 7. It is evident that the two online adaptive ML models significantly outperform their global models across all vehicles in the test set (see Fig. 7a). The online QRNN can deliver the highest accuracy, with a PMAE of 5.04%. Corresponding to a reduction of more than 20% compared to the offline model performance. In comparison with the method proposed in [35], the reduction is as high as 35%. QEGBR, with a PMAE of 5.56%, is also superior to all the global models. Further, for individual trips of a randomly selected vehicle (see Fig. 7b–c), the predicted values of the online adapted QRNN and QEGBR closely follow the ground truth in the entire range of energy consumption. This validates that our proposed online adaptation method can judiciously learn the energy consumption behavior of the target EV and effectively combine it with the corresponding global model.

The effect of online adaption on uncertainty estimation is also investigated. From Table VI, it is clear that the online QRNN and QEGBR effectively reduce the average width of prediction intervals, PI_{AW}, showing a decrease of 15% and 18%, respectively. Similar results are observed in Fig. 8 for individual trips. Obviously, the turquoise-colored areas of the online adaptive models are smaller than the rose-colored areas of the global models. Furthermore, the online QRNN cannot only tighten the prediction intervals but also increase the probability of containing the measured trajectory inside the intervals. This makes its estimated bounds of each prediction

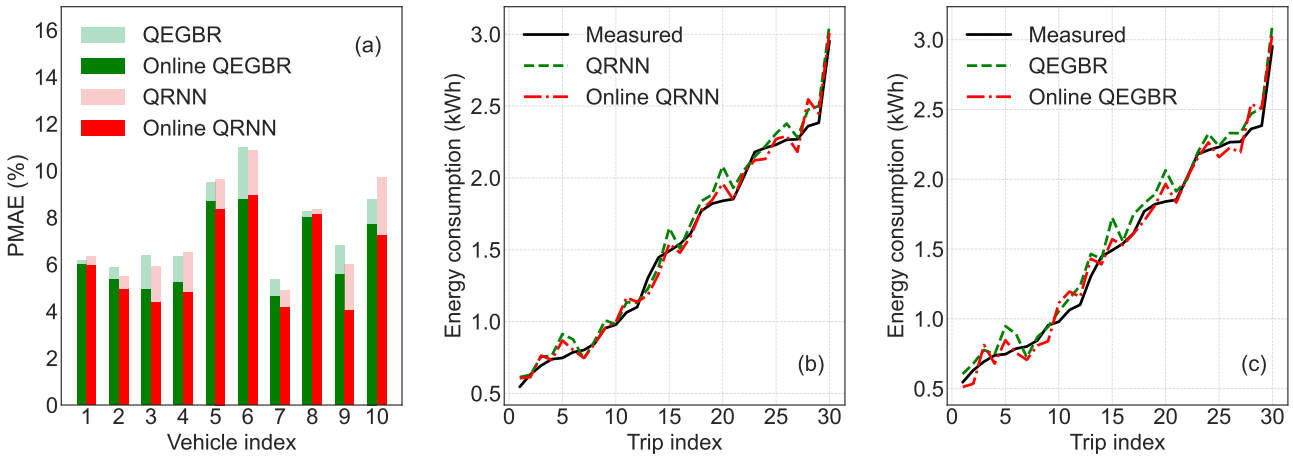

Fig. 7: Comparison of the point prediction results of the global models (QRNN and QEGBR) and their online adaptive models. (a) PMAE values for all vehicles in the test set. (b) and (c) Trajectories of the ground truth and predictions for 30 trips from a randomly selected vehicle in the test set.

TABLE VI: Uncertainty estimation by the global models and online adaptive models

Evaluation matrices	QR	QRF	QRNN	QEGBR	Online QRNN	Online QEGBR
PI_{CP}	0.9354	0.9165	0.8931	0.6377	0.9127	0.5785
PI_{AW}	0.7446	0.6624	0.5981	0.5294	0.5082	0.4348

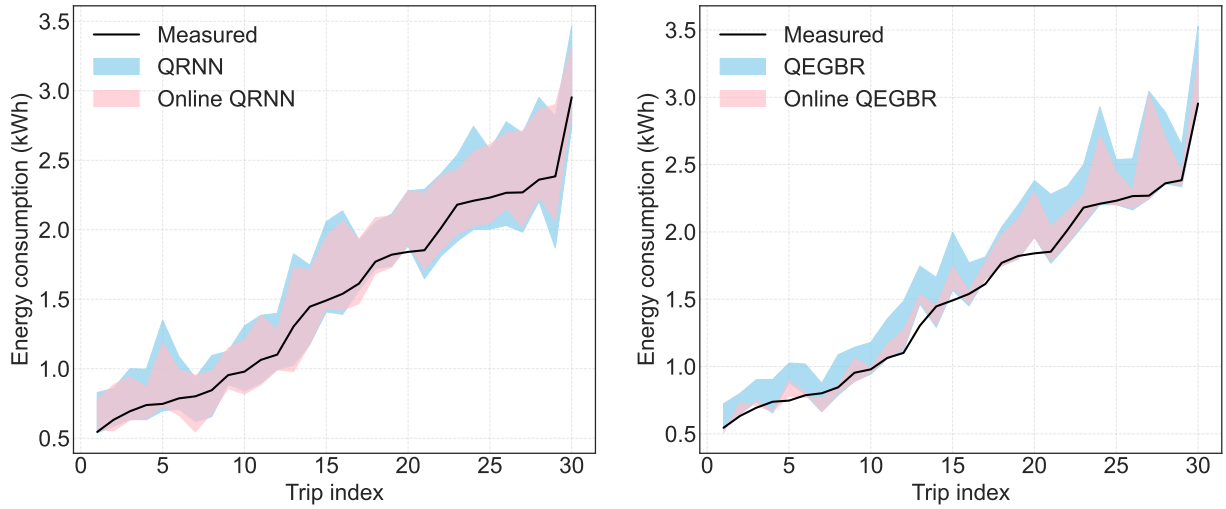

Fig. 8: The estimated uncertainties and the ground truth of energy consumption for a vehicle randomly selected from the test set, where the rose- and turquoise-colored areas denote the 95% prediction intervals.

interval, i.e., $\underline{y}$ and $\overline{y}$, more valuable for advanced EV energy management. By contrast, the online QEGBR shrinks PI_{AW} but also decreases PI_{CP}. Such a low value of PI_{CP} implies that the uncertainty predictions are less reliable and useful.

While significantly enhancing prediction and estimation performance, the online model adaptation will inevitably demand additional computational effort. For instance, when using the online QRNN model, the average computational time is 4.73 milliseconds for predicting the energy consumption of a single trip. This minimal duration makes the developed ML models highly suitable for online vehicular applications.

VI. Conclusions

This paper has introduced a field data-based ML pipeline for the prediction of EV energy consumption. The first novelty arises from the proposed data processing method tailored for a large amount of real-world EV data that was inherently plagued by various issues and outliers. Then, a new feature set was constructed from physical insights and picked meticulously through systematic correlation analyses. Based on these data and features, four quantile-based machine learning algorithms were pertinently formulated and innovatively applied for the EV energy prediction, enabling accurate and reliable prediction of both the energy consumption and associated

uncertainties. Finally, the best-performing global ML models were adapted online for individualized predictions, leading to consistently improved accuracy and tightened confidence internals.

The developed ML models as well as their underpinning data processing and feature engineering were validated extensively for EV energy prediction. Comprehensive comparisons were conducted for different steps of data processing, between global models and online adaptive models, and with models in the literature. The online adaptive QRNN models outperformed all other models with an average prediction error of 5.04%, corresponding to an over 35% improvement over the state-of-the-art models. Substantial advantages have also been observed from different steps of data processing and online model adaptation.

ACKNOWLEDGMENT

The authors would like to thank Prof. Changfu Zou from the Department of Electrical Engineering, Chalmers University of Technology for valuable input and thank Prof. Yi Zhang from the Tsinghua-Berkeley Shenzhen Institute, Tsinghua University for helpful discussions.

REFERENCES

[1] G. J. Offer, "Automated vehicles and electrification of transport," *Energy Environ. Sci.*, vol. 8, no. 1, pp. 26–30, 2015.
[2] E. M. Bibra, E. Connelly, S. Dhir, M. Drtil, P. Henriot, I. Hwang, J.-B. L. Marois, S. McBain, P. Leonardo, and T. Jacob, "Global EV outlook 2022: Securing supplies for an electric future," *Int. Energy Agency*, 2022.
[3] G. Crabtree, "The coming electric vehicle transformation," *Science*, vol. 366, no. 6464, pp. 422–424, 2019.
[4] D. Tan, "Transportation electrification: Challenges and opportunities," *IEEE Power Electron. Mag.*, vol. 3, no. 2, pp. 50–52, 2016.
[5] X. Hu, S. J. Moura, N. Murgovski, B. Egardt, and D. Cao, "Integrated optimization of battery sizing, charging, and power management in plug-in hybrid electric vehicles," *IEEE Trans. Contr. Syst. Technol.*, vol. 24, no. 3, pp. 1036–1043, 2015.
[6] Y. Xu, S. Çolak, E. C. Kara, S. J. Moura, and M. C. González, "Planning for electric vehicle needs by coupling charging profiles with urban mobility," *Nat. Energy*, vol. 3, no. 6, pp. 484–493, 2018.
[7] D. Baek, Y. Chen, A. Bocca, L. Bottaccioli, S. Di Cataldo, V. Gatteschi, D. J. Pagliari, E. Patti, G. Urgese, N. Chang *et al.*, "Battery-aware operation range estimation for terrestrial and aerial electric vehicles," *IEEE Trans. Veh. Technol.*, vol. 68, no. 6, pp. 5471–5482, 2019.
[8] R. Basso, B. Kulcsár, and I. Sanchez-Diaz, "Electric vehicle routing problem with machine learning for energy prediction," *Transp. Res. B*, vol. 145, pp. 24–55, 2021.
[9] Y. Zhang, X. Qu, and L. Tong, "Optimal eco-driving control of autonomous and electric trucks in adaptation to highway topography: Energy minimization and battery life extension," *IEEE Trans. Transport. Electrif.*, vol. 8, no. 2, pp. 2149–2163, 2022.
[10] J. Zhang, T.-Q. Tang, Y. Yan, and X. Qu, "Eco-driving control for connected and automated electric vehicles at signalized intersections with wireless charging," *Appl. Energy*, vol. 282, p. 116215, 2021.
[11] M. Sabri, K. A. Danapalasingam, and M. F. Rahmat, "A review on hybrid electric vehicles architecture and energy management strategies," *Renew. Sustain. Energy Rev.*, vol. 53, pp. 1433–1442, 2016.
[12] G. Correa, P. Muñoz, and C. Rodriguez, "A comparative energy and environmental analysis of a diesel, hybrid, hydrogen and electric urban bus," *Energy*, vol. 187, p. 115906, 2019.
[13] H. Abdelaty, A. Al-Obaidi, M. Mohamed, and H. E. Farag, "Machine learning prediction models for battery-electric bus energy consumption in transit," *Transp. Res. D*, vol. 96, p. 102868, 2021.
[14] M. Xylia, S. Leduc, P. Patrizio, F. Kraxner, and S. Silveira, "Locating charging infrastructure for electric buses in stockholm," *Transp. Res. C*, vol. 78, pp. 183–200, 2017.
[15] L. Li, H. K. Lo, and F. Xiao, "Mixed bus fleet scheduling under range and refueling constraints," *Transp. Res. C*, vol. 104, pp. 443–462, 2019.
[16] A. Desreveaux, A. Bouscayrol, R. Trigui, E. Castex, and J. Klein, "Impact of the velocity profile on energy consumption of electric vehicles," *IEEE Trans. Veh. Technol.*, vol. 68, no. 12, pp. 11 420–11 426, 2019.
[17] X. Wu, D. Freese, A. Cabrera, and W. A. Kitch, "Electric vehicles' energy consumption measurement and estimation," *Transp. Res. D*, vol. 34, pp. 52–67, 2015.
[18] J. Ji, Y. Bie, Z. Zeng, and L. Wang, "Trip energy consumption estimation for electric buses," *Commun. Transp. Res.*, vol. 2, p. 100069, 2022.
[19] C. Zhao, G. Gong, C. Yu, Y. Liu, S. Zhong, Y. Song, C. Deng, A. Zhou, and H. Ye, "Research on key factors for range and energy consumption of electric vehicles," SAE Technical Paper, Tech. Rep., 2019.
[20] G. M. Fetene, S. Kaplan, S. L. Mabit, A. F. Jensen, and C. G. Prato, "Harnessing big data for estimating the energy consumption and driving range of electric vehicles," *Transp. Res. D*, vol. 54, pp. 1–11, 2017.
[21] S. Yang, M. Li, Y. Lin, and T. Tang, "Electric vehicle's electricity consumption on a road with different slope," *Physica A: Stat. Mech. Appl.*, vol. 402, pp. 41–48, 2014.
[22] C. Fiori, K. Ahn, and H. A. Rakha, "Power-based electric vehicle energy consumption model: Model development and validation," *Appl. Energy*, vol. 168, pp. 257–268, 2016.
[23] G. Xia, L. Cao, and G. Bi, "A review on battery thermal management in electric vehicle application," *J. Power Sources*, vol. 367, pp. 90–105, 2017.
[24] X. Yuan, C. Zhang, G. Hong, X. Huang, and L. Li, "Method for evaluating the real-world driving energy consumptions of electric vehicles," *Energy*, vol. 141, pp. 1955–1968, 2017.
[25] O. A. Hjelkrem, K. Y. Lervåg, S. Babri, C. Lu, and C.-J. Södersten, "A battery electric bus energy consumption model for strategic purposes: Validation of a proposed model structure with data from bus fleets in china and norway," *Transp. Res. D*, vol. 94, p. 102804, 2021.
[26] B. Luin, S. Petelin, and F. Al-Mansour, "Microsimulation of electric vehicle energy consumption," *Energy*, vol. 174, pp. 24–32, 2019.
[27] C. Zhang, F. Yang, X. Ke, Z. Liu, and C. Yuan, "Predictive modeling of energy consumption and greenhouse gas emissions from autonomous electric vehicle operations," *Appl. Energy*, vol. 254, p. 113597, 2019.
[28] T. Qian, W. Ming, C. Shao, Q. Hu, X. Wang, J. Wu, and Z. Wu, "An edge intelligence-based framework for online scheduling of soft open points with energy storage," *IEEE Trans. Smart Grid*, vol. 15, no. 3, pp. 2934–2945, 2024.
[29] A. T. Thorgeirsson, S. Scheubner, S. Fünfgeld, and F. Gauterin, "Probabilistic prediction of energy demand and driving range for electric vehicles with federated learning," *IEEE Open J. Veh. Technol.*, vol. 2, pp. 151–161, 2021.
[30] T. Qian, C. Shao, X. Wang, and M. Shahidehpour, "Deep reinforcement learning for ev charging navigation by coordinating smart grid and intelligent transportation system," *IEEE Trans. Smart Grid*, vol. 11, no. 2, pp. 1714–1723, 2019.
[31] T. Qian, Z. Liang, C. Shao, H. Zhang, Q. Hu, and Z. Wu, "Offline drl for price-based demand response: Learning from suboptimal data and beyond," *IEEE Trans. Smart Grid*, 2024.
[32] Y. Chen, Y. Zhang, and R. Sun, "Data-driven estimation of energy consumption for electric bus under real-world driving conditions," *Transp. Res. D*, vol. 98, p. 102969, 2021.
[33] P. Li, Y. Zhang, K. Zhang, and M. Jiang, "The effects of dynamic traffic conditions, route characteristics and environmental conditions on trip-based electricity consumption prediction of electric bus," *Energy*, vol. 218, p. 119437, 2021.
[34] P. Li, Y. Zhang, Y. Zhang, and K. Zhang, "Prediction of electric bus energy consumption with stochastic speed profile generation modelling and data driven method based on real-world big data," *Appl. Energy*, vol. 298, p. 117204, 2021.
[35] J. Zhang, Z. Wang, P. Liu, and Z. Zhang, "Energy consumption analysis and prediction of electric vehicles based on real-world driving data," *Appl. Energy*, vol. 275, p. 115408, 2020.
[36] C. De Cauwer, W. Verbeke, T. Coosemans, S. Faid, and J. Van Mierlo, "A data-driven method for energy consumption prediction and energy-efficient routing of electric vehicles in real-world conditions," *Energies*, vol. 10, no. 5, p. 608, 2017.
[37] Chinese National Technical Committee of Auto Standardization, "Part 3: Communication protocol and data format," *Technical specifications of remote service and management system for electric vehicles*, 2016.
[38] D. Blatná, "Outliers in regression," *Trutnov*, vol. 30, pp. 1–6, 2006.
[39] Y. Zhang, T. Wik, J. Bergström, M. Pecht, and C. Zou, "A machine learning-based framework for online prediction of battery ageing trajectory and lifetime using histogram data," *J. Power Sources*, vol. 526, p. 231110, 2022.

[40] A. Lehman, N. O'Rourke, L. Hatcher, and E. Stepanski, *JMP for basic univariate and multivariate statistics: methods for researchers and social scientists*. Sas Institute Inc., 2013.
[41] R. Koenker and G. Bassett, "Regression quantiles," *Econometrica*, vol. 46, no. 1, pp. 33–50, 1978.
[42] J. W. Taylor, "A quantile regression neural network approach to estimating the conditional density of multiperiod returns," *J. Forecasting*, vol. 19, no. 4, pp. 299–311, 2000.
[43] T. Chen and C. Guestrin, "Xgboost: A scalable tree boosting system," in *Proc. of the 22nd ACM SIGKDD Int. Conf. on Knowledge Discovery and Data Mining*, 2016, pp. 785–794.
[44] Q. Wang, Y. Ma, K. Zhao, and Y. Tian, "A comprehensive survey of loss functions in machine learning," *Ann. Data Sci.*, pp. 1–26, 2020.
[45] C. Chen, "A finite smoothing algorithm for quantile regression," *J. Comput. Graph. Statist.*, vol. 16, no. 1, pp. 136–164, 2007.
[46] N. Meinshausen and G. Ridgeway, "Quantile regression forests." *J. Mach. Learn. Res.*, vol. 7, no. 6, 2006.
[47] Z. Li and D. Hoiem, "Learning without forgetting," *IEEE Trans. Pattern Anal. Mach. Intell.*, vol. 40, no. 12, pp. 2935–2947, 2017.

Qingbo Zhu received the B.S. degree in electrical engineering from Zhengzhou University, Zhengzhou, China, in 2014, and the M.Sc. degree in electrical engineering from Melbourne University, Melbourne, Australia, in 2015. She is currently pursuing the Ph.D. degree in electrical engineering at Chalmers University of Technology, Gothenburg, Sweden. Her research interests primarily involve machine learning algorithms, energy consumption modeling for electric vehicles based on big data, and energy management.

Yicun Huang Dr. Yicun Huang is a Marie Skłodowska-Curie Fellow in the Automatic Control research unit at Chalmers University of Technology. His research focuses on physics-based learning for electrode materials and hazardous reactions within Li-ion battery cells. With a background in computational materials science, his work aims to develop diagnostic algorithms and control strategies to prevent thermal runaway in batteries. One of his research questions involves enhancing conventional, physics-based battery modeling approaches by integrating neural networks for real-time applications.

Chih Feng Lee (Senior Member, IEEE) received the B.E. degree (Hons.) in mechanical and manufacturing engineering and the Ph.D. degree from The University of Melbourne, Melbourne, VIC, Australia, in 2005 and 2014, respectively. His dissertation dealt with the controller design and implementation of a prototype automotive electromechanical brake (EMB), where he explored several model-based control techniques to achieve fast closed-loop clamp force tracking performance. In addition, a novel brake judder attenuation method was proposed, in which EMB was utilized to actively compensate for the judder vibration caused by the variation in thickness around the disk surface. His research activities are centered around developing and applying advanced control techniques to practical problems, where he has a special interest in automotive applications.

Peng Liu (Member, IEEE) received the Ph.D. degree in mechanical engineering from the Beijing Institute of Technology, Beijing, China, in 2011. He is currently an Associate Professor with the School of Mechanical Engineering, Beijing Institute of Technology. His current research interests include battery fault diagnosis, intelligent transportation, and big data analysis

Jin Zhang received the B.S. degree in mechanical engineering from the Beijing Institute of Technology, Beijing, China, in 2016, and the Ph.D. degree in 2023. His research interests primarily involve machine learning algorithms, energy consumption modeling for electric vehicles based on big data, and the locating and capacity planning of electric vehicle charging stations.

Torsten Wik (Member, IEEE) received the M.Sc. degree in chemical engineering, the Licentiate of Engineering degree in control engineering, and the Ph.D. and Docent degrees from the Chalmers University of Technology, Gothenburg, Sweden, in 1994, 1996, 1999, and 2004, respectively. From 2005 to 2007, he worked as a Senior Researcher at Volvo Technology, Gothenburg, in control system design. In 2007, he returned to the Chalmers University of Technology as an Associate Professor, where he is currently a Full Professor and the Head of Automatic Control at the Department of Electrical Engineering. His main research areas are optimal control, process control, and environmentally motivated control applications. During the last decade, the applications have increasingly been focused on battery management systems